Inorganic Chemistry

Article

pubs.acs.org/IC

Modulation of Framework and Centricity: Cation Size Effect in New Quaternary Selenites, $ASc(SeO_3)_2$ (A = Na, K, Rb, and Cs)

Seung Yoon Song and Kang Min Ok*

Department of Chemistry, Chung-Ang University, 84 Heukseok-ro, Dongjak-gu, Seoul 156-756, Republic of Korea

Supporting Information

ABSTRACT: Four new stoichiometrically equivalent quaternary scandium selenites, $ASc(SeO_3)_2$ (A = Na, K, Rb, and Cs) have been hydrothermally synthesized using A_2CO_3, $Sc(NO_3)_3{\cdot}xH_2O$ (or ScO_3), and SeO_2 as starting materials. All four materials share similar bond networks that are composed of corner-shared distorted ScO_6 octahedra and SeO_3 trigonal pyramids. However, each material reveals different frameworks and centricities. Detailed structural analysis suggests that the structural variation is attributed to the difference in size and subsequent coordination number for the alkali metal cations. Powder second-harmonic generation (SHG) measurements on noncentrosymmetric (NCS) $RbSc(SeO_3)_2$ show that the compound has an SHG efficiency similar to that of $(NH_4)H_2PO_4$. The observed SHG efficiency is due to the remaining net polarization after cancellation of oppositely aligned moments for SeO_3 and ScO_6 groups. Thorough characterizations such as spectroscopic, thermal, and elemental analyses for the new materials are presented as are dipole moment and out-of-center distortion calculations.

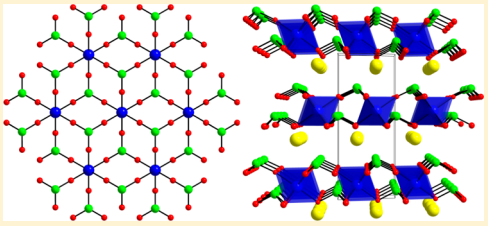

INTRODUCTION

Discovering new solid state materials revealing interesting properties with fascinating structures is an ongoing challenge for synthetic chemists. Among many entrancing materials, those with noncentrosymmetric (NCS) crystal structures have been drawing massive attention owing to their wide range of potential applications to the field of optical communications, sensors, energy harvest, detectors, memories, and so forth.[1] The numerous applications are attributed to their symmetry-dependent properties such as pyroelectricity, ferroelectricity, second-harmonic generation (SHG) behavior, and piezoelectricity.[2] To increase the possibility of creating macroscopic NCS materials, cations with local asymmetric coordination environments have been combined in many synthesis approaches. In synthesizing mixed metal oxide materials, cations susceptible to second-order Jahn−Teller (SOJT) distortions, i.e., lone pair cations (Pb^{2+}, Bi^{3+}, Se^{4+}) and d^0 transition metal cations (Ti^{4+}, V^{5+}, Mo^{6+}) in distortive octahedral environments, have been employed.[3] Other eminent strategies for the formation of NCS materials include incorporation of borates with asymmetric π systems and d^{10} metal cations during the syntheses.[4] In addition, further efforts have been continuously made to rationally design novel NCS materials by understanding the essential elements that affect the overall centricities. A few proven factors exerting influence on the materials' centricities include the cation size, the framework flexibility, and the hydrogen-bonding.[5] We have been systematically investigating mixed metal selenites to prepare novel NCS materials containing the lone pair cation, Se^{4+}. As a versatile starting material, SeO_2 has been extensively utilized in the syntheses of a variety of selenites. In fact, selenium dioxide exhibits excellent reactivity, water solubility, and structural adaptability.[6] Thus, our consistent synthetic endeavors in the A^+−Sc^{3+}−Se^{4+}−oxide (A = Na, K, Rb, and Cs) system resulted in four novel quaternary scandium selenium oxides with a common chemical formula, $ASc(SeO_3)_2$. A number of interesting mixed metal selenites composed of polyhedra of asymmetric moieties have been reported thus far.[7] Several quaternary selenites exhibiting stoichiometry similar to that of the reported materials, i.e., $AM(SeO_3)_2$ (A = alkali metals, M = Y, Ga, and In), have shown rich structural chemistry as well as interesting properties.[5i,8] Here, we are to present the framework modulation and centricity control using the different alkali metal cations in a series of stoichiometrically equivalent selenites. SHG properties for the NCS material will be explained by the net polarization originating from the asymmetric polyhedra.

EXPERIMENTAL SECTION

Reagents. Na_2CO_3 (Hayashi, 99.5%), K_2CO_3 (Jin Chemical, 99.5%), Rb_2CO_3 (Alfa Aesar, 99.8%), Cs_2CO_3 (Aldrich, 99%), $Sc(NO_3)_3{\cdot}xH_2O$ (Acros, 99.9%), Sc_2O_3 (Alfa Aesar, 99.4%), and SeO_2 (Aldrich, 98.0%) were used as received.

Synthesis. Pure single crystals of $ASc(SeO_3)_2$ (A = Na, K, Rb, and Cs) have been grown through hydrothermal reactions. For $NaSc(SeO_3)_2$, 4.00×10^{-3} mol (0.424 g) of Na_2CO_3, 1.30×10^{-3} mol (0.325 g) of $Sc(NO_3)_3{\cdot}xH_2O$, 4.00×10^{-3} mol (0.444 g) of SeO_2, 0.2 mL of HNO_3 (60 wt %), and 2 mL of deionized water were mixed. For $KSc(SeO_3)_2$, 4.00×10^{-3} mol (0.553 g) of K_2CO_3, 1.00×10^{-3} mol (0.249 g) of $Sc(NO_3)_3{\cdot}xH_2O$, 4.00×10^{-3} mol (0.444 g) of SeO_2, 0.2 mL of HNO_3 (60 wt %), and 2 mL of deionized water were mixed. For $RbSc(SeO_3)_2$, 3.00×10^{-3} mol (0.693 g) of Rb_2CO_3, 1.00×10^{-3} mol

Received: March 23, 2015
Published: April 27, 2015

DOI: 10.1021/acs.inorgchem.5b00653
Inorg. Chem. 2015, 54, 5032−5038

Table 1. Crystallographic Data for $ASc(SeO_3)_2$ (A = Na, K, Rb, and Cs)

formula	$NaScSe_2O_6$	$KScSe_2O_6$	$RbScSe_2O_6$	$CsScSe_2O_6$
fw	321.87	337.97	384.35	431.79
space group	*Pnma* (No. 62)	*Pnma* (No. 62)	$P6_3mc$ (No. 186)	*Pnma* (No. 62)
a (Å)	12.8073(4)	13.1696(2)	5.592 90(10)	17.4795(3)
b (Å)	5.4649(2)	5.551 86(13)	5.592 90(10)	5.604 20(10)
c (Å)	8.1408(3)	8.301 17(11)	12.2326(2)	6.991 80(10)
V (Å^3)	569.78(3)	606.95(2)	331.378(15)	684.91(2)
Z	4	4	2	4
T (K)	298.0(2)	298.0(2)	298.0(2)	298.0(2)
λ (Å)	0.710 73	1.5406	0.710 73	0.710 73
ρ_{calcd} (g cm^{-3})	3.752	3.698	3.852	4.188
Flack param	N/A	N/A	−0.012(18)	N/A
$R(F)^a$ or $R_p{}^b$	0.0259	0.0664	0.0198	0.0297
$R_w(F_o{}^2)^c$ or $R_{wp}{}^d$	0.0382	0.0874	0.0351	0.0476

$^aR(F) = \sum||F_o| - |F_c||/\sum|F_o|$. $^bR_p = \sum|I_o - I_c|/\sum I_o$. $^cR_w(F_o{}^2) = [\sum w(F_o{}^2 - F_c{}^2)^2/\sum w(F_o{}^2)^2]^{1/2}$. $^dR_{wp} = [\sum w|I_o - I_c|^2/\sum wI_o{}^2]^{1/2}$.

(0.249 g) of $Sc(NO_3)_3{\cdot}xH_2O$, 4.00 × 10^{-3} mol (0.444 g) of SeO_2, and 1 mL of deionized water were combined. For $CsSc(SeO_3)_2$, 4.00 × 10^{-3} mol (1.303 g) of Cs_2CO_3, 5.00 × 10^{-4} mol (0.069 g) of Sc_2O_3, 8.00 × 10^{-3} mol (0.889 g) of SeO_2, 0.1 mL of HNO_3 (60 wt %), and 10 mL of deionized water were combined. Each reaction mixture was transferred into separate stainless steel autoclaves (23 mL) with Teflon liners. The reactors were sealed tightly and heated to 230 °C for 4 days (180 °C for 3 days for $CsSc(SeO_3)_2$). After heating, the autoclaves were cooled at a rate of 6 °C h^{-1} to room temperature. The autoclaves were opened, and the reaction products were recovered by filtration. After several washings with distilled water, colorless crystals of $NaSc(SeO_3)_2$, $KSc(SeO_3)_2$, $RbSc(SeO_3)_2$, and $CsSc(SeO_3)_2$ were obtained in 66%, 69%, 57%, and 73% yields, respectively, on the basis of starting scandium sources. Obtained crystals of $KSc(SeO_3)_2$ were not appropriate for single crystal X-ray diffraction analysis, although several attempts have been made. Thus, powder X-ray diffraction was utilized to determine the crystal structure of $KSc(SeO_3)_2$. NCS $RbSc(SeO_3)_2$ has been deposited to Noncentrosymmetric Materials Bank (http://ncsmb.knrrc.or.kr).

Single Crystal X-ray Diffraction. A colorless rod with dimensions of 0.010 × 0.010 × 0.101 mm^3 for $NaSc(SeO_3)_2$, a colorless hexagonal bipyramid with dimensions of 0.023 × 0.023 × 0.042 mm^3 for $RbSc(SeO_3)_2$, and a colorless rod with dimensions of 0.007 × 0.010 × 0.060 mm^3 for $CsSc(SeO_3)_2$ were used for single crystal structure determination. A Bruker SMART BREEZE diffractometer with a 1K CCD area detector and monochromated Mo Kα radiation was used at room temperature for the data collection. To acquire the data, a narrow-frame method was used with scan widths of 0.30° in ω and an exposing time of 10 s/frame. For integration of the obtained data, the program SAINT was used.[9] The intensities for collected data were corrected for Lorentz factor, polarization, air absorption, and absorption attributable to the deviation through the detector faceplate in the path length. To make a semiempirical absorption correction on the hemisphere of data, the program SADABS was employed.[10] The data were solved and refined using SHELXS-97 and SHELXL-97, respectively.[11] For all crystallographic calculations, the software package WinGX-98 was used.[12] Important crystallographic data and selected bond distances for the reported compounds are summarized in Tables 1 and 2, respectively.

Powder X-ray Diffraction (PXRD). PXRD data was taken in order to confirm the phase purities of the synthesized materials. The PXRD data were collected on a Bruker D8-Advance diffractometer using Cu Kα radiation at RT with 40 kV and 40 mA. The ground polycrystalline samples were put on sample holders, and the data were obtained in the 2θ range 10−70° with a step size of 0.02° and a step time of 0.2 s. With $KSc(SeO_3)_2$, the diffraction data was analyzed using the Rietveld method with the program GSAS.[13] The refinement was performed with a starting model of the single crystal data of isostructural $NaSc(SeO_3)_2$ in the space group *Pnma*. The measured PXRD patterns for all of the reported materials are in very good agreement with those calculated data from the models obtained from single crystal X-ray diffraction (see the Supporting Information).

Table 2. Selected Bond Distances (Å) for $ASc(SeO_3)_2$ (A = Na, K, Rb, and Cs)

$NaSc(SeO_3)_2$		$KSc(SeO_3)_2$	
Sc(1)−O(1) × 2	2.095(3)	Sc(1)−O(1) × 2	2.145(11)
Sc(1)−O(2)	2.101(4)	Sc(1)−O(2)	2.045(11)
Sc(1)−O(3) × 2	2.112(2)	Sc(1)−O(3) × 2	2.160(8)
Sc(1)−O(4)	2.059(3)	Sc(1)−O(4)	2.205(10)
Se(1)−O(1) × 2	1.683(3)	Se(1)−O(1) × 2	1.693(9)
Se(1)−O(2)	1.685(3)	Se(1)−O(2)	1.658(11)
Se(2)−O(3) × 2	1.689(2)	Se(2)−O(3) × 2	1.715(8)
Se(2)−O(4)	1.679(3)	Se(2)−O(4)	1.788(11)
Na(1)−O(1) × 2	2.811(3)	K(1)−O(1) × 2	2.631(10)
Na(1)−O(2) × 2	2.8808(13)	K(1)−O(2) × 2	2.778(10)
Na(1)−O(3) × 2	2.530(3)	K(1)−O(3) × 2	2.808(9)
Na(1)−O(3) × 2	2.623(3)	K(1)−O(3) × 2	2.895(3)
$RbSc(SeO_3)_2$		$CsSc(SeO_3)_2$	
Sc(1)−O(1) × 3	2.088(6)	Sc(1)−O(1)	2.054(6)
Sc(1)−O(2) × 3	2.108(5)	Sc(1)−O(2) × 2	2.085(4)
Se(1)−O(1) × 3	1.669(6)	Sc(1)−O(3)	2.151(6)
Se(2)−O(2) × 3	1.699(5)	Sc(1)−O(4) × 2	2.137(4)
Rb(1)−O(1) × 3	3.120(6)	Se(1)−O(1)	1.664(6)
Rb(1)−O(2) × 6	3.008(6)	Se(1)−O(2) × 2	1.673(4)
		Se(2)−O(3)	1.691(5)
		Se(2)−O(4) × 2	1.704(4)
		Cs(1)−O(1) × 2	3.492(4)
		Cs(1)−O(2) × 2	3.428(4)
		Cs(1)−O(3) × 2	3.394(3)
		Cs(1)−O(4) × 2	3.103(4)
		Cs(1)−O(4) × 2	3.242(4)

Infrared Spectroscopy. Infrared spectra for the reported materials were recorded on a Thermo Scientific Nicolet iS10 FT-IR spectrometer in the spectral range 400−4000 cm^{-1}, with the well-ground samples intimately contacted by a diamond as an attenuated total reflectance (ATR) crystal.

UV−Vis Diffuse Reflectance Spectroscopy. UV−vis diffuse reflectance spectra were recorded on a Varian Cary 500 scan UV−vis−NIR spectrophotometer over the range 200−2500 nm at room temperature. To convert the reflectance spectra to the absorbance data, the Kubelka−Munk function was used.[14]

Thermogravimetric Analyses (TGA). TGA were carried out using a high-resolution PerkinElmer TGA 7 thermal analyzer. Polycrystalline samples were contained within alumina crucibles and

DOI: 10.1021/acs.inorgchem.5b00653
Inorg. Chem. 2015, 54, 5032−5038

heated at a rate of 10 °C min^{-1} from room temperature to 1000 °C under flowing argon.

Scanning Electron Microscopy/Energy Dispersive Analysis by X-ray (SEM/EDX). SEM/EDX were carried out using a Hitachi S-3400N and a Horiba Energy EX-250 instrument. EDX for $NaSc(SeO_3)_2$, $KSc(SeO_3)_2$, $RbSc(SeO_3)_2$, and $CsSc(SeO_3)_2$ show approximate A:Sc:Se ratios of 1.0:1.0:2.2, 1.0:1.0:2.2, 1.0:0.9:2.0, and 1.0:1.0:2.2, respectively.

Powder Nonlinear Optical (NLO) Measurements. Powder second-harmonic generation (SHG) properties of NCS $RbSc(SeO_3)_2$ were measured by modified Kurtz-NLO system using 1064 nm radiation.[15] The experiments were carried out by a DAWA Q-switched Nd:YAG laser, operating at 20 Hz. A ground polycrystalline sample of $RbSc(SeO_3)_2$ was sieved into distinct particle size ranges to identify the phase-matchability (type 1). Polycrystalline standard samples of α-SiO_2, $(NH_4)H_2PO_4$ (ADP), and $LiNbO_3$ were also sieved into various particle size ranges to compare SHG efficiencies. Powdered samples with particle size range 45−63 μm were used for relevant comparison of SHG efficiencies. Each of the sieved samples with distinct particle sizes was packed into separate capillaries for the SHG measurements in reflection. A 532 nm narrow-pass interference filter was attached to a photomultiplier tube (PMT, Hamamatsu) to prevent the detection of any spurious reflection light. A Tektronix TDS1032 digital oscilloscope was linked to observe the SHG signal. A detailed explanation of the equipment and the method employed was published previously.[1b]

RESULTS AND DISCUSSION

Structures. $NaSc(SeO_3)_2$ and $KSc(SeO_3)_2$. The two alkali metal scandium selenites, $NaSc(SeO_3)_2$ and $KSc(SeO_3)_2$, are isostructural to each other and reveal crystal structures similar to those of $NaIn(SeO_3)_2$ and $KY(SeO_3)_2$.[8] Thus, only a very concise structural explanation of $NaSc(SeO_3)_2$ will be provided here. $NaSc(SeO_3)_2$ crystallizes in the orthorhombic space group *Pnma* (No. 62). The three-dimensional framework of $NaSc(SeO_3)_2$ consists of slightly distorted ScO_6 octahedra and asymmetric SeO_3 groups (see Figure 1). The Sc−O bond distances and the O−Sc−O bond angles in the ScO_6 octahedra range 2.059(3)−2.112(2) Å and 84.07(10)−176.08(14)°, respectively. Two unique Se^{4+} cations also exist in an asymmetric unit with the Se−O bond lengths and O−Se−O bond angles 1.679(3)−1.689(2) Å and 99.08(12)−103.1(2)°, respectively. Finally, the Na^+ cations interact with eight oxygen atoms with the Na−O contact distances 2.530(3)−2.811(3) Å. There are 4-membered ring (4-MR) and 12-membered ring (12-MR) channels obtained along the [010] direction through the corner-sharing of ScO_6 octahedra and SeO_3 trigonal pyramids (see Figure 1). The lone pairs on the SeO_3 groups point toward the inside of the 12-MR channels. Na^+ cations also reside within the 12-MR channels. The connectivity of $NaSc(SeO_3)_2$ may be presented as an anionic framework of $\{[ScO_{6/2}]^{3-}2[SeO_{3/2}]^{1+}\}^-$ with the charge neutrality balanced by the included Na^+. Bond valence sums[16] for the Na^+, Sc^{3+}, Se^{4+}, and O^{2-} are calculated to be 0.84, 3.00, 4.13, and 1.97−2.06, respectively.

$RbSc(SeO_3)_2$. A new quaternary scandium selenite, $RbSc(SeO_3)_2$, crystallizes in the noncentrosymmetric polar hexagonal space group, $P6_3mc$ (No. 186). $RbSc(SeO_3)_2$ exhibits a layered structure consisting of distorted ScO_6 octahedra and SeO_3 polyhedra. The unique cation, Sc^{3+}, is in the octahedral coordination environment, with a cationic displacement in the local C_3 direction that results in three short [2.088(6) Å] and three long [2.108(5) Å] Sc−O bonds. The observed O−Sc−O bond angles are 89.63(14)−179.3(2)°. Within an asymmetric unit, two unique Se^{4+} cations exist, and they are bonded to three oxygen atoms in the SeO_3 trigonal pyramidal moiety with the Se−O bond lengths and the O−Se−O bond angles of 1.669(6)−1.699(5) Å and 100.7(2)−103.3(3)°, respectively. An alkali metal cation, Rb^+, interacts with nine oxygen atoms with Rb−O contact lengths ranging from 3.008(6) to 3.120(6) Å. The ScO_6 octahedron in the center shares all six corners with SeO_3 groups (see Figure 2a). Then, all the corners of SeO_3 trigonal pyramids are linked by the ScO_6 octahedra (see Figure 2b). As seen in Figure 2c, each oxygen in the corners of SeO_3 groups is further connected by the ScO_6 octahedra. The alternating corner-sharing of two kinds of polyhedra continuously expands and forms a hexagonal layer structure. *The*

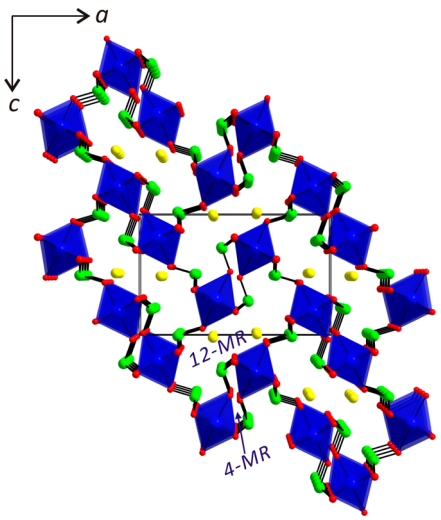

Figure 1. (a) Ball-and-stick and polyhedral representation of $NaSc(SeO_3)_2$ in the *ac*-plane (blue, Sc; green, Se; yellow, Na; red, O). The 4-membered ring (4-MR) and 12-membered ring (12-MR) channels formed through the corner-sharing of ScO_6 octahedra and SeO_3 groups are observed along the [010] direction.

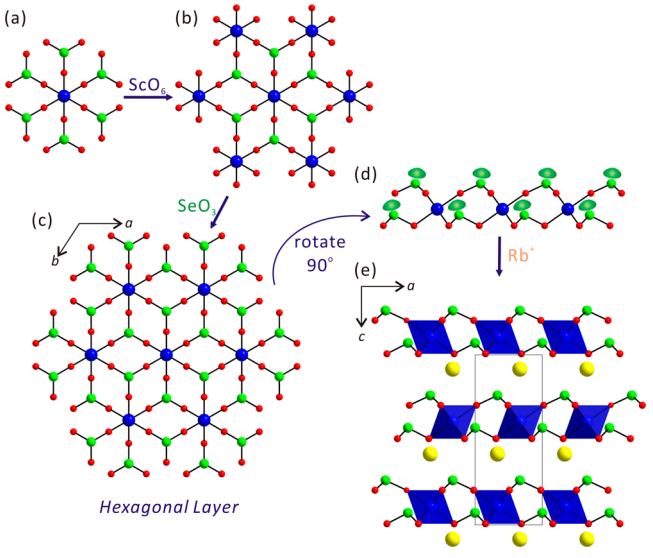

Figure 2. (a) Ball-and-stick representation showing the corner-sharing of a ScO_6 octahedron and six SeO_3 polyhedra in $RbSc(SeO_3)_2$ (blue, Sc; green, Se; red, O). (b) The corners of SeO_3 groups are further shared by ScO_6 octahedra. (c) Further corner-sharing of SeO_3 groups forms a hexagonal layered structure. (d) All the lone pairs on SeO_3 polyhedra are approximately aligned in the [00−1] direction. (e) Rb^+ cations reside in between the layers and complete the whole structure.

DOI: 10.1021/acs.inorgchem.5b00653
Inorg. Chem. 2015, 54, 5032−5038

most interesting structural feature of $RbSc(SeO_3)_2$ is that all of the lone pairs on SeO_3 polyhedra are approximately aligned in the [00−1] direction, which makes the material a polar NCS structure (see Figure 2d). Rb^+ cations reside in between the layers and complete the whole structure of the material (see Figure 2e). In connectivity terms, the backbone of $RbSc(SeO_3)_2$ can be written as an anionic layer of $\{[ScO_{6/2}]^{3-}2[SeO_{3/2}]^{1+}\}^-$ with the overall charge neutrality is maintained by the Rb^+ cation. Bond valence sum calculations[16] for the Rb^+, Sc^{3+}, Se^{4+}, and O^{2-} are 0.95, 2.92, 4.04−4.19, and 2.00−2.03, respectively.

$CsSc(SeO_3)_2$. $CsSc(SeO_3)_2$ is another new quaternary scandium selenite that is crystallizing in the orthorhombic space group, *Pnma* (No. 62). $CsSc(SeO_3)_2$ reveals a three-dimensional framework composed of ScO_6 octahedra and SeO_3 polyhedra. The observed Sc−O bond lengths and O−Sc−O bond angles in the slightly distorted ScO_6 octahedron range from 2.054(6) to 2.151(6) Å and from 86.61(16)° to 176.1(3)°, respectively. The two unique Se^{4+} cations are in an asymmetric trigonal pyramidal coordination environment attributed to the stereoactive lone pairs with the Se−O bond lengths ranging from 1.664(6) to 1.704(4) Å. The huge Cs^+ cation interacts with 10 oxygen atoms with Cs−O contact lengths 3.103(4)−3.492(4) Å. All six corners of the ScO_6 octahedra are shared by the SeO_3 trigonal pyramids through oxygen atoms. In addition, all the corners of the SeO_3 further linked by the ScO_6 through an oxygen atom. The successive Sc−O−Se bonds generate a three-dimensional framework structure with 4-membered ring (4-MR) channels along the [001] direction (see Figure 3a). As seen in Figure 3b, both 4-membered ring (4-MR) and 12-membered ring (12-MR) channels are also monitored along the [010] direction. Within the larger 12-MR channels, Cs^+ cations are situated. Although similar 12-MR channels have been observed previously from $KIn(SeO_3)_2$ or $RbIn(SeO_3)_2$,[8a] the channel geometry of $CsSc(SeO_3)_2$ is slightly different. While the two lone pairs in the longer sides and two lone pairs in the shorter sides point inward within the 12-MR channels in $KIn(SeO_3)_2$, only the two lone pairs in the shorter sides are directed inward in $RbIn(SeO_3)_2$ (see Figure 3c,d). However, the two lone pairs in the longer sides are oriented inward within the 12-MR channels of $CsSc(SeO_3)_2$ (see Figure 3b). The framework of $CsSc(SeO_3)_2$ can be written as $\{[ScO_{6/2}]^{3-}2[SeO_{3/2}]^{+}\}^-$ with the charge balance retained by the Cs^+ cation. Bond valence sum calculations[16] for the Cs^+, Sc^{3+}, Se^{4+}, and O^{2-} turn out to be 0.91, 2.87, 4.02−4.17, and 1.95−2.05, respectively.

Infrared (IR) Spectroscopy. IR spectroscopy has been utilized to be sure of the existence of the particular bonding in the reported compounds. The IR spectra for $ASc(SeO_3)_2$ (A = Na, K, Rb, and Cs) present Sc−O and Se−O vibrations. Bands found around 411−491 cm^{-1} may be attributable to Sc−O vibrations, whereas multiple peaks observed between 524 and 916 cm^{-1} are due to Se−O vibrations. The IR vibrations and assignments for all four reported compounds are listed in Table 3. The peak assignments are in agreements with those reported materials.[5i,8,17]

UV−Vis Diffuse Reflectance Spectroscopy. To extract band gaps for the reported solid state materials, the UV−vis diffuse reflectance spectra have been measured. The (K/S)-versus-E plots obtained from the calculations using the Kubelka−Munk function[14] reveal band gaps for $NaSc(SeO_3)_2$, $KSc(SeO_3)_2$, $RbSc(SeO_3)_2$, and $CsSc(SeO_3)_2$ at about 5.5, 5.4, 4.9, and 5.2 eV, respectively. The observed band gaps may be attributable to the extent of Sc (3d) orbital participation in the conduction bands as well as the deformations arising from SeO_3 groups in the variable channel geometries.

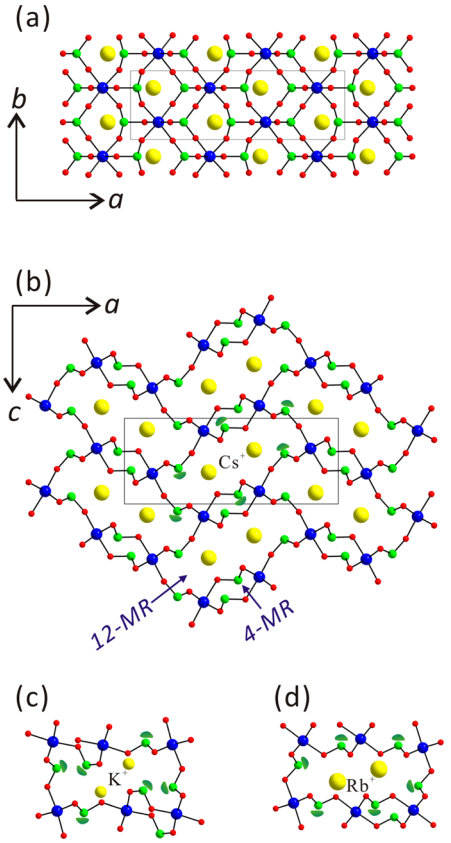

Figure 3. Ball-and-stick models revealing a three-dimensional framework structure of $CsSc(SeO_3)_2$ (a) in the *ab*-plane and (b) in the *ac*-plane (yellow, Cs; blue, Sc; green, Se; red, O). Both 4-MR and 12-MR channels are also observed along the [010] direction. Ball-and-stick representations showing 12-MR channels found from (c) $KIn(SeO_3)_2$ and (d) $RbIn(SeO_3)_2$. Note the different orientations of lone pairs on SeO_3 polyhedra.

Table 3. Infrared Vibrations (cm^{-1}) for $ASc(SeO_3)_2$ (A = Na, K, Rb, and Cs)

compd	Sc−O	Se−O
$NaSc(SeO_3)_2$	418, 483	714, 759, 839, 857, 869, 879
$KSc(SeO_3)_2$	411, 475	541, 557, 633, 715, 813, 859, 875, 885
$RbSc(SeO_3)_2$	421, 491	556, 631, 705, 746, 895, 916
$CsSc(SeO_3)_2$	421, 449, 478	524, 535, 713, 737, 803, 864, 880

Thermal Analysis. Thermogravimetric analyses have been carried out to examine the thermal stabilities of the reported selenites. $NaSc(SeO_3)_2$, $KSc(SeO_3)_2$, $RbSc(SeO_3)_2$, and $CsSc(SeO_3)_2$ are thermally stable up to 600, 640, 620, and 600 °C, respectively. No weight losses have been observed from the TGA diagrams. Powder X-ray diffraction patterns obtained at different temperatures confirm the stabilities of the materials at higher temperatures (see the Supporting Information). Once temperatures increase further, the materials decompose to mixtures of corresponding alkali metal selenites (A_2SeO_4, A = Na, K, Rb, and Cs), Sc_2O_3, and SeO_2 attributed to the sublimation of SeO_2. The decompositions are identified by PXRD data measured on thermally decomposed products for $ASc(SeO_3)_2$ at 1000 °C in air.

DOI: 10.1021/acs.inorgchem.5b00653
Inorg. Chem. 2015, 54, 5032−5038

Powder Second-Harmonic Generation (SHG) Measurements. One of the reported materials, $RbSc(SeO_3)_2$, crystallizes in an NCS polar space group. Powder SHG measurements with 1064 nm radiation show that $RbSc(SeO_3)_2$ has an SHG efficiency similar to that of $(NH_4)H_2PO_4$ (ADP). Further measurements on the sieved polycrystalline samples with several different particle size ranges suggest that $RbSc(SeO_3)_2$ is non-phase-matchable (type 1) and can be categorized as a class C SHG material (see Figure 4).[15] The

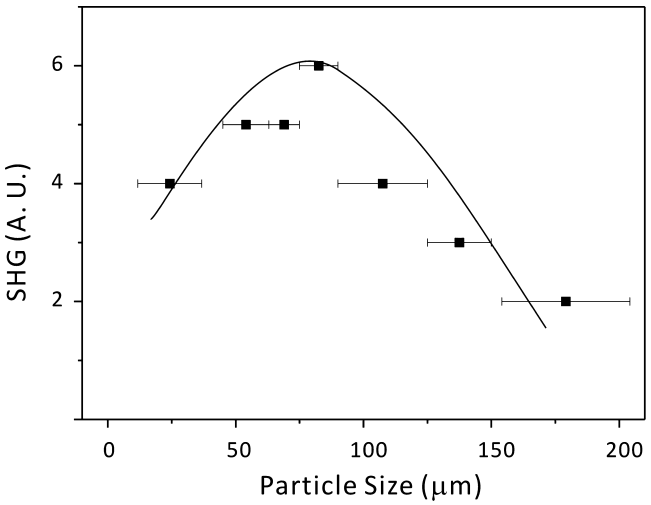

Figure 4. Phase matching (type I) curve for NCS $RbSc(SeO_3)_2$. The curve is to guide the eye and is not a fit to the data.

measured SHG efficiency for $RbSc(SeO_3)_2$ can be justified by analyzing the net polarization deriving from the individual local asymmetric units. As seen in Figure 5, a unique Sc^{3+} and two unique Se^{4+} cations with unsymmetrical coordination environments exist within an asymmetric unit of $RbSc(SeO_3)_2$. As we described earlier, the Sc^{3+} cation exhibits a cationic displacement toward a face and results in three short and three long Sc−O bonds. More specifically, the three short Sc(1)−O(1) bonds [2.088(6) Å] point toward the approximate [00−1] direction, whereas the three long Sc(1)−O(2) bonds [2.108(5) Å] direct to the approximate [001] direction. Thus, a net moment is generated toward the [00−1] direction attributed to the distorted ScO_6 octahedron. Meanwhile, another net moment is also expected from asymmetric SeO_3 polyhedra with lone pairs. The lone pairs on both $Se(1)^{4+}$ and $Se(2)^{4+}$ cations approximately point to the [00−1] direction although they are slightly tilted. Since the moment directs toward the opposite direction of the lone pair, the polarization associated with Se^{4+} cations occurs to the [001] direction. Then, the moments arising from ScO_6 and SeO_3 are directed in opposite directions. As we will explain in more detail later, the dipole moment for ScO_6 is smaller than that of SeO_3 (see Dipole Moment Calculations section). Thus, a net polarization occurs parallel to the [001] direction when the moments are taken as a whole (see Figure 5). The observed weak SHG efficiency for $RbSc(SeO_3)_2$ is mainly attributed to the cancellation of oppositely aligned moments. In addition, the pink color of polycrystalline $RbSc(SeO_3)_2$ may hinder the detection of SHG light.

Dipole Moment and Out-of-Center Distortions Calculations. All of the reported materials are composed of asymmetric polyhedra such as distorted ScO_6 octahedra and

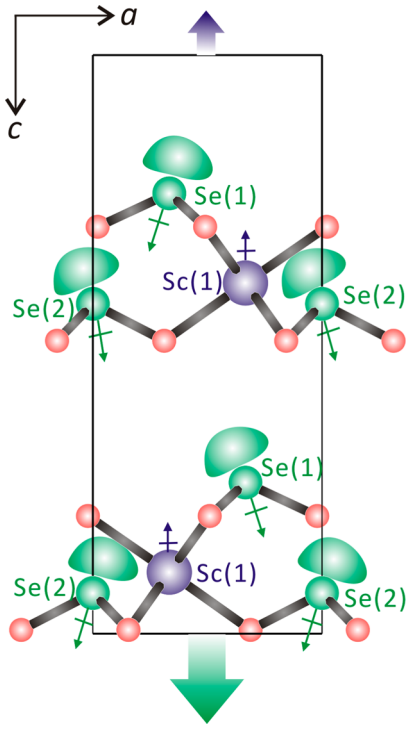

Figure 5. Ball-and-stick representation showing the net moment arising from ScO_6 octahedra and SeO_3 polyhedra in $RbSc(SeO_3)_2$. A moment is generated toward the [00−1] direction attributed to the C_3 cationic displacement of ScO_6 octahedron. Another moment attributable to the alignment of lone pairs on Se^{4+} is also observed in the [001] direction. When taken as a whole, a small net moment is observed along the [001] direction. The lone pair on Se^{4+} is drawn schematically and is not the result of the electron localization function (ELF) calculations.

SeO_3 trigonal pyramids. Thus, more detailed analyses on the extent of distortions of the asymmetric polyhedra may help to better understand the coordination modes of the materials regardless of their centricities. With $RbSc(SeO_3)_2$, it would be very helpful to quantify the direction and magnitude of the distortions to explain the origin of the SHG efficiency. Therefore, the local dipole moments for the asymmetric polyhedra in the reported materials have been investigated using a bond valence sum.[18] The dipole moments for the ScO_6 and SeO_3 groups are calculated to be about 0.4−2.7 and 5.7−8.2 D (D = Debyes), respectively, which are quite similar to those previously reported values.[5i,j,17,19] As we will discuss more in detail later, the different local dipole moment values for ScO_6 octahedra are attributable to the magnitudes of octahedral distortions influenced by the interactions between different alkali metal cations and oxide ligands. A complete list of the calculated dipole moments for the corresponding polyhedra is tabulated in Table 4.

With the ScO_6 octahedra in the reported materials, the magnitude of out-of-center distortions (Δ_d's) can also be quantified using the method described before.[20] The calculated Δ_d values for ScO_6 groups in $NaSc(SeO_3)_2$, $KSc(SeO_3)_2$, $RbSc(SeO_3)_2$, and $CsSc(SeO_3)_2$ are 0.08, 0.19, 0.06, and 0.18, respectively, which are similar to those of previously reported ScO_6 octahedra.[21] On the basis of the calculated Δ_d, ScO_6 octahedra can be classified as weak distorters.

Effect of Cation Size on the Frameworks and Centricities. All four reported materials, $ASc(SeO_3)_2$ (A =

DOI: 10.1021/acs.inorgchem.5b00653
Inorg. Chem. 2015, 54, 5032−5038

Table 4. Calculation of Dipole Moments for ScO_6 and SeO_3 Polyhedra[a]

compd	species	dipole moment (D)
$NaSc(SeO_3)_2$	$Se(1)O_3$	8.2
	$Se(2)O_3$	7.6
	$Sc(1)O_6$	2.5
$KSc(SeO_3)_2$	$Se(1)O_3$	5.7
	$Se(2)O_3$	7.5
	$Sc(1)O_6$	2.7
$RbSc(SeO_3)_2$	$Se(1)O_3$	7.0
	$Se(2)O_3$	7.8
	$Sc(1)O_6$	0.4
$CsSc(SeO_3)_2$	$Se(1)O_3$	6.9
	$Se(2)O_3$	7.9
	$Sc(1)O_6$	2.6

[a]D = Debyes.

Na, K, Rb, and Cs), are stoichiometrically similar; however, each compound containing a different alkali metal reveals a dissimilar framework geometry. In addition, while $ASc(SeO_3)_2$ (A = Na, K, and Cs) crystallize in CS space groups, $RbSc(SeO_3)_2$ exhibits a polar NCS space group. Both $NaSc(SeO_3)_2$ and $KSc(SeO_3)_2$ containing smaller ionic radii (8-coordinate Na^+, 1.18 Å; 8-coordinate K^+, 1.51 Å)[22] interact with eight oxygen atoms. Therefore, the 12-MR channels contain the smaller alkali metal cations as well as the lone pairs on the SeO_3 polyhedra (see Figure 6a). Similar channel structures have been monitored from $NaIn(SeO_3)_2$ and $KIn(SeO_3)_2$.[8a] $RbSc(SeO_3)_2$ with relatively larger Rb^+ cations (9-coordinate Rb^+, 1.63 Å)[22] reveals 2D layers attributed to the larger interlayer spacing (see Figure 6b). It should be noticed that the stoichiometrically similar rubidium indium selenite, $RbIn(SeO_3)_2$, exhibits a 3D structure with 12-MR channels.[8a] The structural variance between $RbSc(SeO_3)_2$ and $RbIn(SeO_3)_2$ seems to be the consequence of the different framework flexibilities. Whereas the larger flexible InO_6 octahedra along with the SeO_3 can encompass Rb^+ cations within the 12-MR channels in $RbIn(SeO_3)_2$, the similar channel structure is not possible in $RbSc(SeO_3)_2$ that contains the small rigid ScO_6 octahedra. Also, directional contacts of the Rb^+ cation with nine oxygen atoms in ScO_6 and SeO_3 have $RbSc(SeO_3)_2$ to crystallize in a polar NCS space group. Finally, $CsSc(SeO_3)_2$ reveals another type of 3D channel structure. More close structural examinations suggest that the 12-MR channel in $CsSc(SeO_3)_2$ has been achieved by the larger coordination number of Cs^+ cation (10-coordinate Cs^+, 1.81 Å)[22] that can interact with 10 oxygen atoms in ScO_6 and SeO_3 polyhedra (see Figure 6c). Each layer has been shifted to opposite directions, and the SeO_3 groups can link the layers to maintain the 12-MR channels.

CONCLUSIONS

A series of new alkali metal scandium selenium oxides, $ASc(SeO_3)_2$ (A = Na, K, Rb, and Cs) have been prepared in phase pure forms through hydrothermal reactions. Isostructural $NaSc(SeO_3)_2$ and $KSc(SeO_3)_2$ show three-dimensional framework structures with 4- and 12-MR channels. NCS $RbSc(SeO_3)_2$ shows an aligned layered structure that is composed of the corner-shared distorted ScO_6 octahedra and asymmetric SeO_3 trigonal pyramids. $CsSc(SeO_3)_2$ reveals another 3D channel structure with different orientation of lone pairs on SeO_3 polyhedra. The structural variances and dissimilar

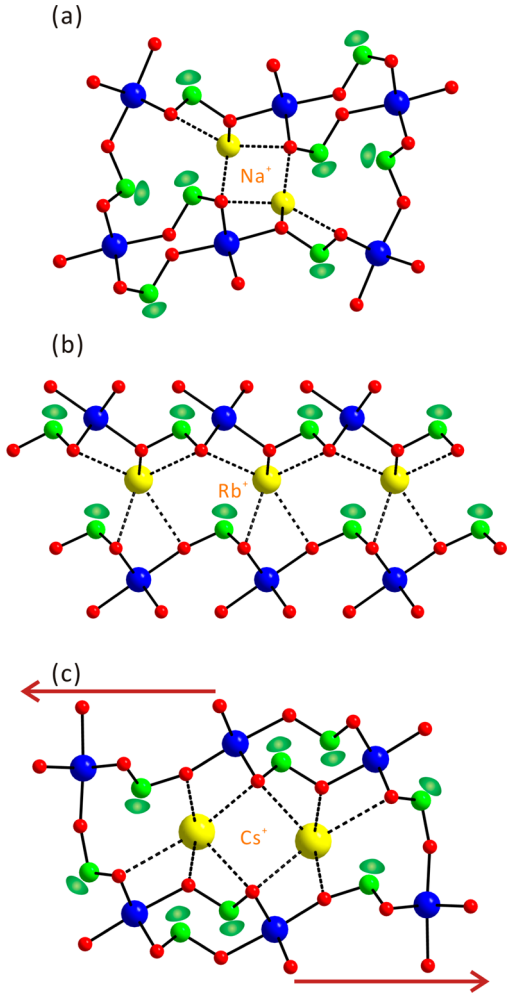

Figure 6. Ball-and-stick models representing the effect of the cation size on the frameworks and centricities in (a) $NaSc(SeO_3)_2$, (b) $RbSc(SeO_3)_2$, and (c) $CsSc(SeO_3)_2$ (yellow, Na, Rb, or Cs; blue, Sc; green, Se; red, O).

centricities for the stoichiometrically equivalent materials are attributable to the different size of alkali metal cations and the variable coordination environments. Powder SHG measurements with 1064 nm radiation reveal that NCS $RbSc(SeO_3)_2$ is non-phase-matchable (Type 1) and has a similar SHG efficiency to that of ADP. Detailed structural examinations suggest that the measured SHG is attributed to a net moment deriving from the aligned lone pairs on Se^{4+}.

ASSOCIATED CONTENT

Supporting Information

X-ray crystallographic file in CIF format, calculated and observed X-ray diffraction patterns, thermogravimetric analysis diagrams, infrared spectra, and UV−vis diffuse reflectance spectra for $ASc(SeO_3)_2$ (A = Na, K, Rb, and Cs). The Supporting Information is available free of charge on the ACS Publications website at DOI: 10.1021/acs.inorgchem.5b00653.

AUTHOR INFORMATION

Corresponding Author

*E-mail: kmok@cau.ac.kr. Phone: +82-2-820-5197. Fax: +82-2-825-4736.

DOI: 10.1021/acs.inorgchem.5b00653
Inorg. Chem. 2015, 54, 5032−5038

Notes

The authors declare no competing financial interest.

■ ACKNOWLEDGMENTS

This work was supported by the National Research Foundation of Korea (NRF) grant funded by the Korea government (MSIP) (nos. 2013R1A2A2A01007170 and 2014M3A9B8023478). This research was also supported by the Chung-Ang University Freshmen Academic Record Excellent Scholarship Grants in 2014 (for S.Y.S.).

■ REFERENCES

(1) (a) Nye, J. F. *Physical Properties of Crystals*; Oxford University Press: Oxford, U.K., 1957. (b) Ok, K. M.; Chi, E. O.; Halasyamani, P. S. *Chem. Soc. Rev.* **2006**, *35*, 710−717.

(2) (a) Jona, F.; Shirane, G. *Ferroelectric Crystals*; Pergamon Press: Oxford, U.K., 1962;. (b) Cady, W. G. *Piezoelectricity; An Introduction to the Theory and Applications of Electromechanical Phenomena in Crystals*; Dover: New York, 1964. (c) Lang, S. B. *Sourcebook of Pyroelectricity*; Gordon & Breach Science: London, U.K., 1974.

(3) (a) Opik, U.; Pryce, M. H. L. *Proc. R. Soc. London* **1957**, *A238*, 425−447. (b) Bader, R. F. W. *Can. J. Chem.* **1962**, *40*, 1164−1175. (c) Pearson, R. G. *J. Am. Chem. Soc.* **1969**, *91*, 4947−4955. (d) Pearson, R. G. *THEOCHEM* **1983**, *103*, 25−34. (e) Wheeler, R. A.; Whangbo, M.-H.; Hughbanks, T.; Hoffmann, R.; Burdett, J. K.; Albright, T. A. *J. Am. Chem. Soc.* **1986**, *108*, 2222−2236. (f) Oh, S.-J.; Shin, Y.; Tran, T. T.; Lee, D. W.; Yoon, A.; Halasyamani, P. S.; Ok, K. M. *Inorg. Chem.* **2012**, *51*, 10402−10407.

(4) (a) Pan, S.; Smit, J. P.; Watkins, B.; Marvel, M. R.; Stern, C. L.; Poeppelmeier, K. R. *J. Am. Chem. Soc.* **2006**, *128*, 11631−11634. (b) Jiang, H.; Kong, F.; Fan, Y.; Mao, J.-G. *Inorg. Chem.* **2008**, *47*, 7430−7437. (c) Wu, H.; Pan, S.; Poeppelmeier, K. R.; Li, H.; Jia, D.; Chen, Z.; Fan, X.; Yang, Y.; Rondinelli, J. M.; Luo, H. *J. Am. Chem. Soc.* **2011**, *133*, 7786−7790. (d) Shi, Y.; Pan, S.; Dong, X.; Wang, Y.; Zhang, M.; Zhang, F.; Zhou, Z. *Inorg. Chem.* **2012**, *51*, 10870−10875. (e) Wang, L.; Pan, S.; Chang, L.; Hu, J.; Yu, H. *Inorg. Chem.* **2012**, *51*, 1852−1858. (f) Hao, Y.-C.; Hu, C.-L.; Xu, X.; Kong, F.; Mao, J.-G. *Inorg. Chem.* **2013**, *52*, 13644−13650. (g) Xu, X.; Hu, C.-L.; Kong, F.; Zhang, J.-H.; Mao, J.-G.; Sun, J. *Inorg. Chem.* **2013**, *52*, 5831−5837. (h) Yang, B.-P.; Hu, C.-L.; Xu, X.; Huang, C.; Mao, J.-G. *Inorg. Chem.* **2013**, *52*, 5378−5384. (i) Fan, X.; Zang, L.; Zhang, M.; Qiu, H.; Wang, Z.; Yin, J.; Jia, H.; Pan, S.; Wang, C. *Chem. Mater.* **2014**, *26*, 3169−3174. (j) Song, J.-L.; Hu, C.-L.; Xu, X.; Kong, F.; Mao, J.-G. *Angew. Chem., Int. Ed.* **2015**, *54*, 3679−3682.

(5) (a) Sykora, R. E.; Ok, K. M.; Halasyamani, P. S.; Albrecht-Schmitt, T. E. *J. Am. Chem. Soc.* **2002**, *124*, 1951−1975. (b) Goodey, J.; Ok, K. M.; Broussard, J.; Hofmann, C.; Escobedo, F. V.; Halasyamani, P. S. *J. Solid State Chem.* **2003**, *175*, 3−12. (c) Ok, K. M.; Baek, J.; Halasyamani, P. S.; O'Hare, D. *Inorg. Chem.* **2006**, *45*, 10207−10214. (d) Chang, H.-Y.; Kim, S.-H.; Ok, K. M.; Halasyamani, P. S. *J. Am. Chem. Soc.* **2009**, *131*, 6865−6873. (e) Choi, M.-H.; Kim, S.-H.; Chang, H. Y.; Halasyamani, P. S.; Ok, K. M. *Inorg. Chem.* **2009**, *48*, 8376−8382. (f) Lee, D. W.; Bak, D.-b.; Kim, S. B.; Kim, J.; Ok, K. M. *Inorg. Chem.* **2012**, *51*, 7844−7850. (g) Lee, D. W.; Oh, S. J.; Halasyamani, P. S.; Ok, K. M. *Inorg. Chem.* **2012**, *50*, 4473−4480. (h) Oh, S.-J.; Lee, D. W.; Ok, K. M. *Inorg. Chem.* **2012**, *51*, 5393−5399. (i) Lee, D. W.; Ok, K. M. *Inorg. Chem.* **2013**, *52*, 5176−5184. (j) Kim, Y. H.; Lee, D. W.; Ok, K. M. *Inorg. Chem.* **2014**, *53*, 1250−1256. (k) Kim, Y. H.; Thao, T. T.; Halasyamani, P. S.; Ok, K. M. *Inorg. Chem. Front.* **2015**, *2*, 361−368.

(6) Lide, D. R. *CRC Handbook of Chemistry and Physics*, Internet Version 2005; CRC Press: Boca Raton, FL, 2005.

(7) (a) Harrison, W. T. A.; Dussack, L. L.; Jacobson, A. J. *Inorg. Chem.* **1994**, *33*, 6043−6049. (b) Vaughey, J. T.; Harrison, W. T. A.; Dussack, L. L.; Jacobson, A. J. *Inorg. Chem.* **1994**, *33*, 4370−4375. (c) Porter, Y.; Halasyamani, P. S. *J. Solid State Chem.* **2003**, *174*, 441−449. (d) Sivakumar, T.; Chang, H. Y.; Baek, J.; Halasyamani, P. S. *Chem. Mater.* **2007**, *19*, 4710−4715. (e) Chang, H. Y.; Kim, S. W.; Halasyamani, P. S. *Chem. Mater.* **2010**, *22*, 3241−3250. (f) Li, P. X.; Kong, F.; Hu, C. L.; Zhao, N.; Mao, J.-G. *Inorg. Chem.* **2010**, *49*, 5943−5952.

(8) (a) Lee, D. W.; Kim, S. B.; Ok, K. M. *Inorg. Chem.* **2012**, *51*, 8530−8537. (b) Bang, S.-e.; Lee, D. W.; Ok, K. M. *Inorg. Chem.* **2014**, *53*, 4756−4762.

(9) *SAINT, A Program for Area Detector Absorption Correction, version 4.05*; Siemens Analytical X-ray Instruments: Madison, WI, 1995.

(10) Blessing, R. H. *Acta Crystallogr., Sect. A* **1995**, *51*, 33−38.

(11) (a) Sheldrick, G. M. *SHELXS-97—A Program for Automatic Solution of Crystal Structures*; University of Goettingen: Goettingen, Germany, 1997. (b) Sheldrick, G. M. *SHELXL-97—A Program for Crystal Structure Refinement*; University of Goettingen: Goettingen, Germany, 1997.

(12) Farrugia, L. J. *J. Appl. Crystallogr.* **1999**, *32*, 837−838.

(13) Larson, A. C.; von Dreele, R. B. *General Structural Analysis System (GSAS)*; Los Alamos National Laboratory: Los Alamos, NM, 1987.

(14) (a) Kubelka, P.; Munk, F. *Z. Tech. Phys.* **1931**, *12*, 593. (b) Tauc, J. *Mater. Res. Bull.* **1970**, *5*, 721−729.

(15) Kurtz, S. K.; Perry, T. T. *J. Appl. Phys.* **1968**, *39*, 3798−3813.

(16) (a) Brown, I. D.; Altermatt, D. *Acta Crystallogr., Sect. B* **1985**, *41*, 244−247. (b) Brese, N. E.; O'Keeffe, M. *Acta Crystallogr., Sect. B* **1991**, *47*, 192−197.

(17) Song, S. Y.; Lee, D. W.; Ok, K. M. *Inorg. Chem.* **2014**, *53*, 7040−7046.

(18) (a) Galy, J.; Meunier, G. *J. Solid State Chem.* **1975**, *13*, 142−159. (b) Maggard, P. A.; Nault, T. S.; Stern, C. L.; Poeppelmeier, K. R. *J. Solid State Chem.* **2003**, *175*, 27−33. (c) Izumi, H. K.; Kirsch, J. E.; Stern, C. L.; Poeppelmeier, K. R. *Inorg. Chem.* **2005**, *44*, 884−895.

(19) Lee, D. W.; Oh, S.-J.; Halasyamani, P. S.; Ok, K. M. *Inorg. Chem.* **2011**, *50*, 4473−4480.

(20) Halasyamani, P. S. *Chem. Mater.* **2004**, *16*, 3586−3592.

(21) Kim, Y. H.; Lee, D. W.; Ok, K. M. *Inorg. Chem.* **2013**, *52*, 11450−11456.

(22) Shannon, R. D. *Acta Crystallogr.* **1976**, *A32*, 751−767.

DOI: 10.1021/acs.inorgchem.5b00653
Inorg. Chem. 2015, 54, 5032−5038